https://doi.org/10.17221/218/2016-SWR

Measurement and Computation of Kinetic Energy of Simulated Rainfall in Comparison with Natural Rainfall

Jan PETRŮ and Jana KALIBOVÁ*

Department of Land Use and Improvement, Faculty of Environmental Sciences, Czech University of Life Sciences Prague, Prague, Czech Republic

**Corresponding author: jpetru@fzp.czu.cz*

Abstract

Petrů J., Kalibová J. (2018): Measurement and computation of kinetic energy of simulated rainfall in comparison with natural rainfall. Soil & Water Res., 13: 226–233.

Rainfall characteristics such as total amount and rainfall intensity (*I*) are important inputs in calculating the kinetic energy (*KE*) of rainfall. Although *KE* is a crucial indicator of the raindrop potential to disrupt soil aggregates, it is not a routinely measured meteorological parameter. Therefore, *KE* is derived from easily accessible variables, such as *I*, in empirical laws. The present study examines whether the equations which had been derived to calculate *KE* of natural rainfall are suitable for the calculation of *KE* of simulated rainfall. During the experiment presented in this paper, the measurement of rainfall characteristics was carried out under laboratory conditions using a rainfall simulator. In total, 90 measurements were performed and evaluated to describe the rainfall intensity, drop size distribution and velocity of rain drops using the Thies laser disdrometer. The duration of each measurement of rainfall event was 5 minutes. Drop size and fall velocity were used to calculate *KE* and to derive a new equation of time-specific kinetic energy ($KE_{time} - I$). When comparing the newly derived equation for *KE* of simulated rainfall with the six most commonly used equations for $KE_{time} - I$ of natural rainfall, *KE* of simulated rainfall was discovered to be underestimated. The higher the rainfall intensity, the higher the rate of underestimation. *KE* of natural rainfall derived from theoretical equations exceeded *KE* of simulated rainfall by 53–83% for $I = 30$ mm/h and by 119–275% for $I = 60$ mm/h. The underestimation of *KE* of simulated rainfall is probably caused by smaller drops formed by the rainfall simulator at higher intensities (94% of all drops were smaller than 1 mm), which is not typical of natural rainfall.

Keywords: disdrometer; drop size distribution; rainfall intensity; rainfall simulator

Soil erosion is a mechanical process of land degradation caused by natural and anthropogenic factors, which has a negative impact on underlying soil functions. The soil is the basis for food and biomass production and plays a crucial role as a habitat for biota and as a gene pool. Moreover, it stores, filters, buffers and transforms a large variety of substances, including water, inorganic and organic compounds (Blum *et al.* 2006).

Rainfall simulators were developed to enable the application of torrential rainfall anywhere and anytime while ensuring the utmost control of rainfall characteristics such as their spatial and temporal variability, intensity, duration, terminal velocity of the falling drops, drop size distribution (DSD), kinetic energy of rainfall and repeatability of the simulated rainfall (Thomas & El Swaify 1989; Dunkerley 2008).

The total kinetic energy of rainfall (*KE*) is used as an indicator of the potential ability of rain to disrupt soil aggregates and it essentially represents the sum of kinetic energy of the rain drops falling on the ground (Salles *et al.* 2002; Van Dijk 2002). According to Fornise (2005), the kinetic energy of rainfall may be expressed in two ways: as time-specific kinetic energy and volume-specific kinetic

https://doi.org/10.17221/218/2016-SWR

energy. Time-specific kinetic energy is calculated per unit area per unit time. In this study, it is reported as KE_{time} (J/m^2/h). Volume-specific kinetic energy of rain (J/m^2/mm) is expressed as the rainfall depth per unit area and is indicated KE_{mm}.

It is indisputable and widely recognized that information about rainfall kinetic energy is very significant for all studies of soil erosion. Despite this fact, *KE* is not a routinely measured meteorological parameter. The main reason is that kinetic energy is complicated to measure due to its temporal and spatial variability and that expensive and sophisticated instruments are required (Fornis *et al.* 2005).

One way to determine the kinetic energy of rainfall is to derive it from measured drop size distribution (DSD) and terminal fall velocity of rain drops (v_t) or through empirical laws linking the drop diameter (D) and v_t. To determine DSD, it is necessary to know the size of raindrops (D).

The other way to obtain the value of kinetic energy as its derivation from rainfall intensity. The rainfall intensity is a commonly and easily measurable meteorological variable in most countries. This allows the determination of the relationship between kinetic energy and rain intensity. This relationship cannot be generally applied in all countries, because of the site-specific character of the origin and type of precipitation (Rosewell 1986; McIsaac 1990; Jayawardene & Rezaur 2000; Petan *et al.* 2010; Sanchez-Moreno *et al.* 2012; Angulo-Martínez & Barros 2015). Linear and power-law relationships are the most commonly used mathematical expressions of the relationship between time-specific kinetic energy and rainfall intensity ($KE_{time} – I$). Exponential or logarithmic relationships seem to be the most suitable for a description of the relationship between volume-specific kinetic energy and rainfall intensity ($KE_{mm} – I$) (Sanchez-Moreno *et al.* 2012).

The aim of this study was to compare two approaches to quantification of the kinetic energy of rainfall: (1) determination of *KE* on the basis of DSD and drop fall velocity and (2) derivation of *KE* from the equation of $KE_{time} – I$. The main question this study is supposed to answer is to what extent the kinetic energy of simulated rainfall corresponds with the kinetic energy of natural rainfall.

MATERIAL AND METHODS

The experiment was carried out in the laboratory of the Faculty of Environmental Sciences, University of Life Sciences in Prague. The Norton Ladder Rainfall Simulator was used to simulate the rain. This apparatus was developed by Dr D. Norton at the USDA, Agricultural Research Service, National Soil Erosion Research Laboratory, West Lafayette, USA. The drop formers used for the Norton simulator are four Spraying Systems Veejet 80100 nozzles. The study experiment was carried out using a single nozzle. Plastic barriers were placed on the edges of the experimental plot to prevent an overlap from the neighbouring nozzles. The simulator operates at a pressure of 41 kPa, which allows 14.75 l/min of water flow through each nozzle and along with the fall height it is reported to provide rainfall characteristics similar to a natural rain – 2.3 mm median drop size and comparable kinetic energy (Meyer & McCune 1958; Bubenzer 1979). The intensity control of the simulator is based on a timing circuit that controls the sweep frequency of the oscillating mechanism. The more the nozzle sweeps, the higher the rainfall intensity. The nozzle sweep frequency is controlled from a stand-alone controller.

To estimate rainfall characteristics a laser precipitation monitor (LPM) – disdrometer by the Thies Company was used (Fernández-Raga *et al.* 2010; Frasson *et al.* 2011; Iserloh *et al.* 2013). LPM works on the principle of the laser ray interruption by falling raindrops, with the sampling area of 228 × 20 mm. LPM is designed to measure the maximum rainfall intensity of 250 mm/h, the size of raindrops from 0.125 to 8 mm and drop fall velocity 2–20 m/s. The device divides raindrops into 22 classes based on drop diameter (Table 1). Rainfall characteristics (intensity, drop size distribution, drop fall velocity) were determined from 5-minute rainfall events; final values refer to 1-minute period. No other specific validation methods (than LPM records) were used to validate the rainfall characteristics. LPM shows

Table 1. Particle diameter classes

Class	Diameter (mm)	Class	Diameter (mm)	Class	Diameter (mm)
1	≥ 0.125	9	≥ 1.75	17	≥ 5.5
2	≥ 0.250	10	≥ 2	18	≥ 6
3	≥ 0.375	11	≥ 2.5	19	≥ 6.5
4	≥ 0.5	12	≥ 3	20	≥ 7
5	≥ 0.75	13	≥ 3.5	21	≥ 7.5
6	≥ 1	14	≥ 4	22	≥ 8
7	≥ 1.25	15	≥ 4.5		
8	≥ 1.5	16	≥ 5		

https://doi.org/10.17221/218/2016-SWR

good reproducibility, which is due to the fact that it records all drops throughout the entire size range. In contrast, for example, the Joss-Waldvogel disdrometer records only a small portion of rainfall volume, which has an impact on measurement accuracy. Therefore, LPM is recommended as the best tool for the measurement of rainfall characteristics (Ries *et al.* 2009). LPM detailed description can be found in Fernández-Raga *et al.* (2010) or Thies (2004). The vertical distance of the nozzle from the LPM was 2 m.

For better coverage of rainfall spatial variability, the LPM was located at three positions under the simulator (Figure 1). Positions were selected based on the evaluation of the spatial distribution of rainfall to the places of the highest, lowest and average rainfall intensity. The spatial distribution of the simulated rainfall was evaluated by the collecting cups method and next by a calculation of the Christiansen coefficient of uniformity (CU). Collecting cups were placed on the experimental plot in a square grid with a cell size 0.1 m; in total, 100 collecting cups were installed. This method was described in detail by Iserloh *et al.* (2013) or Ries *et al.* (2009). The measurements were carried out for all ten preset intensity modes (rainfall intensity ranged from 17 mm/h to 126 mm/h) of the simulator in order to get a detailed description of the range of intensities provided by the simulator. During the experiment, the LPM was

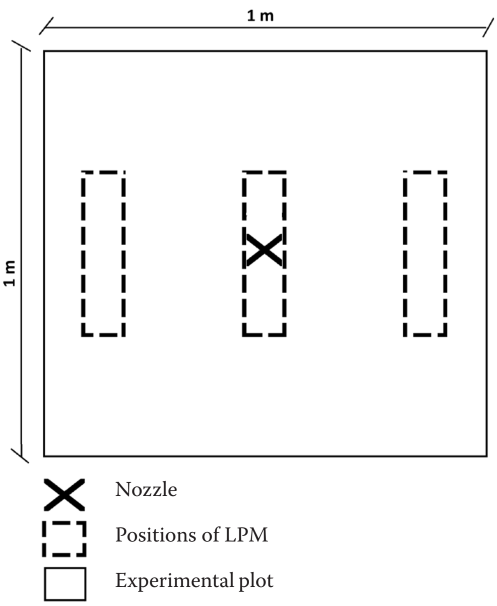

Figure 1. Position of a laser precipitation monitor (LPM) above the experimental plot (square shaped plot, size 1 × 1 m)

placed into three positions; three replications were used. In total, 90 measurements were evaluated to record simulated rainfall characteristics in detail. The duration of each measurement was 5 minutes.

Calculation of kinetic energy and relationship between KE_{time} and I. Rainfall kinetic energy was calculated using the equation by Fornis *et al.* (2005). This equation was derived for disdrometer RD-80, but it can also be applied for the Thies LPM. Values of time-specific kinetic energy (KE_{time}, J/m^2/h) for each 1-minute event were calculated using Eq. (1):

$$KE_{\text{time}} = \left(\frac{\pi}{12}\right)\left(\frac{1}{10^6}\right)\left(\frac{3600}{t}\right)\left(\frac{1}{A}\right)\sum_{i=1}^{22} n_i D_i^3 \left(v_{D_i}\right)^2 \quad (1)$$

where:

A – sampling area of the LPM (0.005 m^2)
t – rainfall duration (60 s)
n_i – number of drops in the class of individual diameter range (–)
D_i – drop class diameter (mm)
v_{Di} – fall velocity of drops (m/s) of the diameter D_i (mm)

Although KE is a crucial indicator of the raindrop potential to disrupt soil aggregates, it is not a routinely measured meteorological parameter, neither are the rainfall characteristics such as drop size or fall velocity. Therefore, KE is derived from easily accessible variables, such as I, in empirical laws. A specific equation to calculate the kinetic energy of simulated rainfall, based on measurements of DSD and fall velocity in laboratory conditions, was derived and provided in the technical documentation of the LPM. This equation (Eq. (1)) was used to calculate KE of the individual rainfall intensities (preset by the simulator control unit) simulated in this study. Then we calculated KE of the simulated rainfall intensities using the empirical laws which had been derived for natural rainfall (Eq. (2)–(7) in Table 2). As input data, only the rainfall intensity was used. Finally, we compared the values of KE calculated based on (1) drop size and fall velocity (equation for simulated rainfall) and (2) rainfall intensity (empirical law for natural rainfall).

To this purpose, six equations were chosen which are derived from the relation of rainfall kinetic energy and rainfall intensity (Table 2). The equations were chosen to cover all continents (except Australia) and represent logarithmic, exponential, power-law and linear equations expressing the kinetic energy of rainfall.

Based on the results, a new equation for the calculation of KE of simulated rainfall was derived (Eq. (8)

https://doi.org/10.17221/218/2016-SWR

Table 2. Some established relationships between kinetic energy content (KE_{time}, J/m^2/h) and rainfall intensity (I, mm/h) for different countries

Eq. No.	Reference	Equation KE_{time}	Location
(2)	Wischmeier and Smith (1978)	I (11.87 + 8.73 log$I$)	North America
(3)	Jayawardena and Rezaur (2000)	36.8I [1 – 0.691 exp(–0.038I)]	Hong Kong
(4)	Steiner and Smith (2000)	11$I^{1.25}$	Northern Mississippi, USA
(5)	Hudson (1965)	29.86(I – 4.29)	Zimbabwe
(6)	Zanchi and Torri (1980)	I (9.81 + 11.25log$I$)	Italy
(7)	Van Dijk (2002)	28.3I [1 – 0.52 exp(–0.042I)]	world

and Eq. (9)). In this equation, only rainfall intensity (commonly measured rainfall characteristic) serves as input data. This equation is supposed to be more suitable to calculate *KE* of simulated rainfall than the empirical laws which had been derived for *KE* of natural rainfall.

RESULTS AND DISCUSSION

In total, 90 measurements were carried out with a range of intensity from 15.9 mm/h to 172.3 mm/h. The average intensity of rainfall was 58.6 mm/h, KE_{time} = 706.6 J/m^2/h. The median drop diameter of all measurements was measured to range from 0.375 to 0.5 mm, which is less than the values described by Iserloh *et al.* (2013) or Ries *et al.* (2009). The mean drop size and fall velocity measured by LPM are depicted in Figure 2. It is evident from the percentage of the number of drops in individual size classes that 85% of drops fall into the first four classes with maximum drop diameter 0.75 mm (for the range of size classes see Table 1), and 90.5% of drops fall into the first five classes (maximum drop diameter 1 mm). Assoulinea *et al.* (1997), Cerdà *et al.* (1997), Clarke and Walsh (2007), Ries *et al.* (2009), Iserloh *et al.* (2012, 2013) reported that in their studies most drops were smaller than 1 mm. Smaller drops are probably formed due to the construction of the driven nozzle simulator. In here, the rainfall intensity is determined by the number of sweeps, the pressure remains unchanged. The drop size does not change with the increasing rainfall intensity. This does not correspond to natural conditions. Our results do not directly confirm the statement that the Veejet

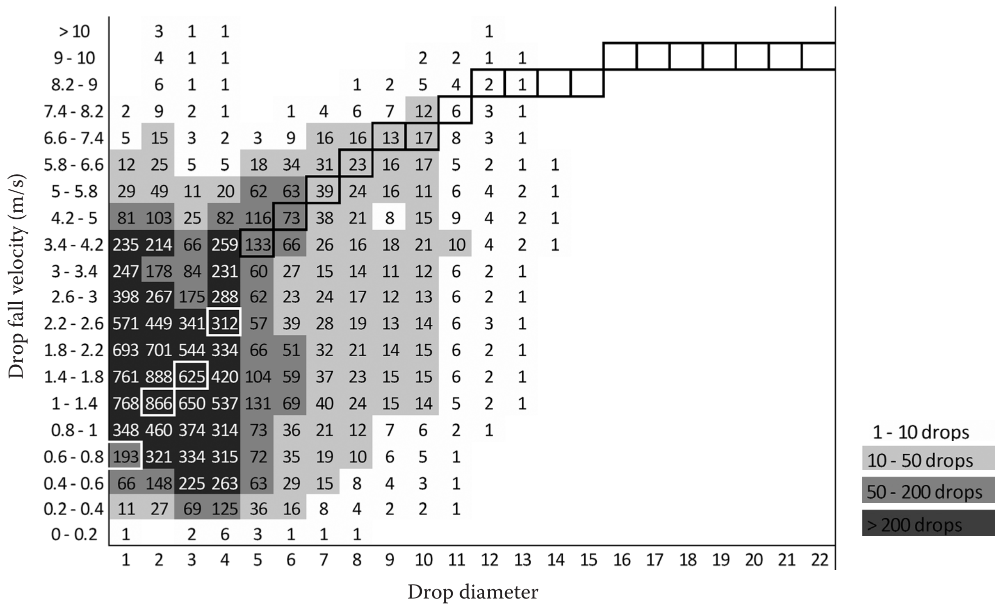

Figure 2. Average results of drop size distribution (DSD) and drop fall velocity measured by a laser precipitation monitor (LPM), mean values representing 1 min simulated rainfall (average from all measurements); drop diameter and corresponding fall velocities for vertical natural rainfall in calm conditions are marked with a red frame (Iserloh *et al.* 2012)

https://doi.org/10.17221/218/2016-SWR

80100 nozzles by the Spraying Systems Company produce the rainfall of characteristics which are similar to the characteristics of natural rainfall. It might be worth using different types of nozzles in further research to find out whether better rainfall characteristics (closer to the natural ones) may be simulated. Higher values of median volumetric drop diameters were reported by Fister *et al.* (2012), Shelton *et al.* (1985). In this study, another issue to be discussed was the spatial distribution of rainfall. The distribution was evaluated using a method of collecting cups. After the rainfall event, the amount of rainfall water in each cup was evaluated and the mean value of rainfall amount (in one cup / point of the test plot) was determined. In terms of the spatial distribution of rainfall, the maximum deviation of the rainfall amount (from the mean value of rainfall amount) in individual cups (point of the test plot) equalled 90%. The reason for such deviation might be the physical characteristics of the nozzles and potential fluctuations in water pressure. However, the good Christiansen coefficient of uniformity CU = 80% (average from all measurements) ensures the quality of the spatial distribution of simulated rainfall. Esteves *et al.* (2000) reported that the values of Christiansen coefficient should reach at least 80% to provide good reproducibility of the spatial distribution of rainfall.

Comparison of KE_{time} measured and calculated by the relation KE_{time} – I. Relations between the range of values of time-specific kinetic energy (KE_{time}, J/m²/h) and rainfall intensity were obtained by regression analysis and expressed by two mathematical expressions – by power law and logarithmic relationships. The fitted power-law equation is Eq. (8):

$$KE_{time} = 50.633(I)^{0.656},\ R^2 = 0.8 \tag{8}$$

And the fitted logarithmic equation is Eq. (9):

$$KE_{time} = -1195.7 + 483.181\ln(I),\ R^2 = 0.81 \tag{9}$$

The relation $KE_{time} – I$ in the power-law equation is provided in Figure 3. Eq. (8) tends to overestimate KE_{time} at rainfall intensity up to 10 mm/h. For I = 10–15 mm/h, KE_{time} is comparable with other equations. At rainfall intensity higher than 15 mm/h, KE_{time} is gradually underestimated when compared with other equations (Figure 4). For I = 30 mm/h, the value of KE_{time} underestimates the values from other equations by 53–83%. For I = 60 mm/h, the values are higher by 119–275%. The Eq. (9) provides better R^2. However, when using the logarithmic expression which is more suitable for KE_{time}, negative values of KE_{time} appear for rainfall intensities lower than 10 mm/h. For intensities higher than 10 mm/h, Eq. (9) provides similar or slightly lower values than Eq. (8). For this reason, only Eq. (8) was later used to compare $KE_{time} – I$ derived in laboratory conditions with equations of $KE_{time} – I$ derived from natural rainfall. The equations used for the comparison were derived for different ranges of rainfall intensities and different climatic and morphological conditions.

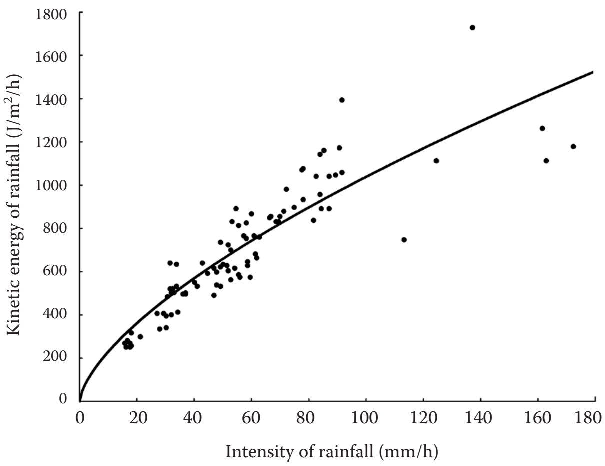

Figure 3. The scatter plot of time-specific kinetic energy equation ($KE_{time} – I$) data and the fitted power-law relation (Eq. (8))
KE_{time} – time-specific kinetic energy; I – rainfall intensity

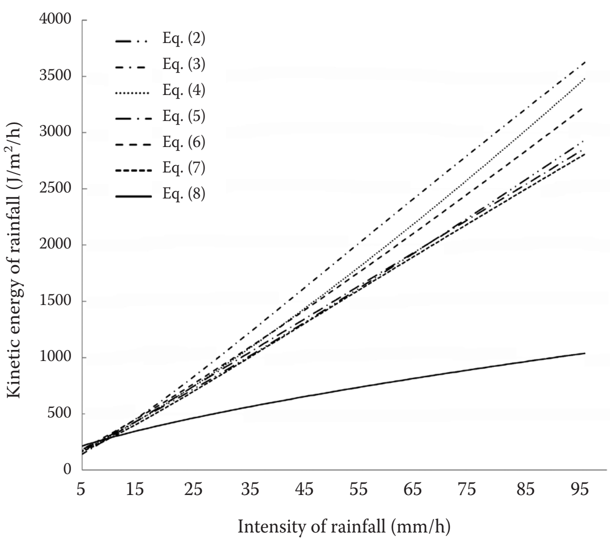

Figure 4. Comparison of time-specific kinetic energy (KE_{time}) calculated according to different equations of $KE_{time} – I$
I – rainfall intensity

https://doi.org/10.17221/218/2016-SWR

Table 3. Basic statistics of examined equations, including the statistics of significant thresholds for particular mean values, α = 0.05 (in $J/m^2/h$)

Eq. No.	Mean	SD	SE	95% confidence interval for mean		Min	Max
				lower bound	upper bound		
(8)	839	351	64	708	970	145	1354
(2)	2250	1395	255	1729	2771	90	4630
(3)	2737	1694	309	2105	3370	79	5507
(4)	2663	1761	322	2006	3321	82	5774
(5)	2186	1314	240	1695	2677	21	4351
(6)	2475	1557	284	1893	3056	88	5144
(7)	2139	1286	235	1658	2619	82	4241

SD – standard deviation; SE – standard error

Table 3 shows the basic statistics of examined relations $KE_{\text{time}} - I$, such as mean, minimum and maximum KE_{time}. Eq. (8) provides the lowest values of individual characteristics, except the minimum value. The graphical comparison of all tested equations is given in Figure 4.

For an objective comparison of the examined equations, a single-factor ANOVA balanced model was used, which firstly determines the statistical significance of the differences between the results of individual equations (Table 4). The Fisher-Snedecor distribution was used to determine the statistical significance of the differences between individual equations. Secondly, after meeting the basic conditions, a post-hoc analysis was used to determine statistically significant differences between individual equations (Table 5).

A group of seven equations was divided into two homogeneous groups. More sensitive Tukey's HSD parametric method was used to test statistically significant differences indicated by ANOVA. This method showed Eq. (8) to be different at a significance level of α = 0.05. Less sensitive Scheffe's method determined Eq. (8) and Eq. (7) to belong to the first group.

Table 5. Results of post-hoc analysis to demonstrate statistical significance of differences between individual equations

Eq. No.	Subset for α = 0.05	
	1	2
Tukey HSD		
(8)	839	
(7)		2139
(5)		2186
(2)		2250
(6)		2475
(4)		2663
(3)		2737
Scheffe		
(8)	839	
(7)	2139	2139
(5)		2186
(2)		2250
(6)		2475
(4)		2663
(3)		2737

CONCLUSIONS

This study aimed to (1) determine the kinetic energy of simulated rainfall on the basis of measured drop size distribution and fall velocity and (2) compare this method with 6 commonly used equations of $KE_{\text{time}} - I$. Data analysis showed that:

– 94% of drops of the simulated rainfall were smaller than 1 mm. Drop speed of smaller drops is overestimated and the speed of large drops is underestimated compared to natural rain. However, the overall trend of rain drop fall velocity is increasing. The intensity of simulated rainfall increased through rising drop density and the frequency of their impact, not through increasing drop size.

– On the basis of the relation $KE_{\text{time}} - I$, a new Eq. (8) was derived to determine *KE* of simulated rainfall. For this reason, it is not suitable to be used to de-

Table 4. Results of ANOVA analysis, including the test of statistical significance of the testing criterion *F* (Fisher-Snedecor distribution) for results of kinetic energy (*KE*) calculation by different equations

	Sum of squares	df	Mean square	*F*	Significance
Between groups	73 043 331	6	12 173 888	6.15	0.000
Within groups	401 564 670	203	1 978 151		
Total	474 608 000	209			

df – degree of freedom

https://doi.org/10.17221/218/2016-SWR

termine *KE* of natural rainfall. Eq. (8) is suitable to be used to determine *KE* of simulated rainfall, especially for the type of simulator and nozzle used in the present study.

– Simulator nozzles are supposed to provide kinetic energy which is at 80% similar to natural rainfall (Humphrey *et al*. 2002). However, the kinetic energy of simulated rainfall is strongly underestimated (in comparison with equations derived for natural rainfall). For I = 30 mm/h, Eq. (2) – Eq. (7) overestimate KE_{time} by 53–83%. For I = 60 mm/h, calculated KE_{time} surpasses measured *KE* by 119–175%. However, this underestimation is not caused by a wrong form of the equations (they might still work well for natural rainfall), but by different characteristics of the simulated rainfall (smaller drops are produced). This should be kept in mind when choosing a proper equation to calculate the *KE* of simulated rainfall.

– The newly derived power-law equation for the calculation of simulated rainfall KE_{time} is comparable with other equations up to rainfall intensity 15 mm/h. For higher intensities, the KE_{time} is gradually underestimated. According to Tuckey's test, there is a statistically significant difference between Eq. (8) and Eq. (2) – Eq. (7) at a significance level of $\alpha = 0.05$.

Results show significant differences between kinetic energy of simulated rainfall and natural rainfall, which should be taken into account when deciding whether to use the $KE_{\text{time}} - I$ relation (derived from natural rainfall events) for description of simulated rainfall. When compared to natural rainfall, the KE of simulated rainfall seems to be underestimated at higher rainfall intensities. The reason probably lies in the difference in the size of drops of natural and simulated rainfall – in natural rainfall there is a trend of increasing drops with the overall rainfall intensity, while in simulated rainfall the drop diameter is rather constant through the whole range of preset intensity (the intensity is increased by more frequent sweeps under the same water pressure). Thus, the expected results of potential soil loss under simulated rainfall conditions should reach lower values than during natural rainfall events. In other words, at the same intensity rates, simulated rainfall should generate lower KE and therefore a lower disruption of the soil surface than natural rainfall does.

Acknowledgements. This experiment was supported by the Internal Grant Agency of the Czech University of Life Sciences in Prague, Faculty of Environmental Sciences, Grant IGA No. 42190/1312/423142. The authors are grateful to their colleagues from the Department of Land Use and Improvement, and especially to Prof. M. Janecek, for their help.

References

Angulo-Martínez M., Barros A.P.O.D. (2015): Measurement uncertainty in rainfall kinetic energy and intensity relationships for soil erosion studies: An evaluation using PARSIVEL disdrometers in the Southern Appalachian Mountains. Geomorphology, 228: 28–40.

Assoulinea S., El Idrissib A., Persoons E. (1997): Modelling the physical characteristics of simulated rainfall: a comparison with natural rainfall. Journal of Hydrology, 266: 336–447.

Blum W.E.H., Warkentin B.P., Frossard E. (2006): Soil, human society and the environment. Geological Society, Special Publication, 266: 1–8.

Bubenzer G.D. (1979): Rainfall characteristics important for simulation. In: Proc. Rainfall Simulator Workshop, Tuscon, March 7–9, 1979, U.S. Department of Agriculture Science and Education Administration Agricultural Reviews and Manuals, ARM –W-10/July1979.

Cerdà A., Ibáñez S., Calvo A. (1997): Design and operation of small and portable rainfall simulator for rugged terrain. Soil Technology, 11: 161–168.

Clarke M.A., Walsh R.P.D. (2007): A portable rainfall simulator for field assessment of splash and slopewash in remote locations. Earth Surface Processes Landforms, 32: 2052–2069.

Dunkerley D. (2008): Rain event properties in nature and in rainfall simulation experiments: a comparative review with recommendations for increasingly systematic study and reporting. Hydrological Processes, 22: 4415–4435.

Esteves M., Planchon O., Lapetite J.M., Silvera N., Cadet P. (2000): The „EMIRE" large rainfall simulator: design and field testing. Earth Surface Processes Landforms, 25: 681–690.

Fernandéz-Raga M., Fraile R., Keizer J.J., Teijeiro M.E.V., Castro A., Palencia C., Calvo A.I., Koenders J., Marques R.L.C. (2010): The kinetic energy of rain measured with an optical disdrometer: An application to splash erosion. Atmospheric Research, 96: 225–240.

Fister W., Iserloh T., Ries J.B., Schmidt R.G. (2012): A portable wind and rainfall simulator for in situ soil erosion measurements. Catena, 91: 72–84.

Fornis R.L., Vermeulen H.R., Nieuwenhuis J.D. (2005): Kinetic energy-rainfall intensity relationship for Central Cebu, Philippines for soil erosion studies. Journal of Hydrology, 300: 20–32.

Frasson R.P.M., Cunha L.K., Krajewski W.K. (2011): Assessment of the Thies optical disdrometer performance. Atmospheric Research, 101: 237–255.

https://doi.org/10.17221/218/2016-SWR

Hudson N.W. (1965): The influence of rainfall mechanics on soil erosion. [Ph.D. Thesis.] Cape Town, University of Cape Town.

Humphrey J.B., Daniel T.C., Edwards D.R., Sharpley A.N. (2002): A portable rainfall simulator for plot-scale runoff studies. Applied Engineering in Agriculture, 18: 199–204.

Iserloh T., Fister W., Seeger M., Willger H., Ries J.B. (2012): A small portable rainfall simulator for reproducible experiments on soil erosion. Soil & Tillage Research, 124: 131–137.

Iserloh T., Ries J.B., Arnáez J., Boix-Fayos C., Butzen V., Cerdà A., Echeverría M.T., Fernández-Gálvez J., Fister W., Geißler C., Gómez J.A., Gómez-Macpherson H., Kuhn N.J., Lázaro R., León F.J., Martínez-Mena M., Matrínez-Murillo J.F., Marze M., Mingorance M.D., Ortigosa L., Peters P., Regüé D., Ruiz-Sinoga J.D., Scholten T., Seeger M., Solé-Benet A., Wengel R., Wirtz S. (2013): European small portable rainfall simulator: A comparison of rainfall chracteristics. Catena, 110: 100–112.

Jayawardena A.W., Rezaur R.B. (2000): Drop size distribution and kinetic energy load of rainstorms in Hong Kong. Hydrological Processes, 14: 1069–1082.

McIsaac G.F. (1990): Apparent geographic and atmospheric influences on raindrop sizes and rainfall kinetic energy. Journal of Soil and Water Conservation, 45: 663–666.

Meyer L., McCune D.L. (1958): Rainfall simulator for runoff plots. Agricultural Engineering, 39: 644–648.

Petan S., Rusjan S., Vidmar A., Mikoš M. (2010): The rainfall kinetic energy-intensity relationship for rainfall erosivity estimation in the mediterranean part of Slovenia. Journal of Hydrology, 391: 314–321.

Ries J.B., Seeger M., Iserloh T., Wistorf S., Fister W. (2009): Calibration of simulated rainfall characteristics for the study of soil erosion on agricultural land. Soil & Tillage Research, 106: 109–116.

Rosewell C.J. (1986): Rainfall kinetic energy in eastern Australia. Journal of Climate and Applied Meteorology, 25: 1695–1701.

Salles Ch., Poesen J., Sempere-Torres D. (2002): Kinetic energy of rain and its functional relationship with intensity. Journal of Hydrology, 257: 256–270.

Sanchez-Moreno J.F., Mannaerts Ch.M., Jetten V., Löffler-Mang M. (2012): Rainfall kinetic energy-intensity and rainfall momentum-intensity relationships for Cape Verde. Journal of Hydrology, 454–455: 131–140.

Shelton C.H., von Bernuth R.D., Rajbhandari S.P. (1985): A continuous-application rainfall simulator. Transactions of the ASAE, 28: 1115–1119.

Steiner M., Smith J.A. (2000): Reflectivity, rain rate, and kinetic energy flux relationships based on raindrop spectra. Journal of Climate and Applied Meteorology, 39: 1923–1940.

Thies (2004): Instruction for use 021341/07/11 Laser Precipitation Monitor 5.4110.xx.x00 V2.5x STD. Göttingen, Adolf Thies GmbH & Co KG.

Thomas N.P., El Swaify S.A. (1989): Construction and calibration of rainfall simulator. Journal of Agricultural Engineering Research, 43: 1–9.

Van Dijk A.M. (2002): Rainfall intensity-kinetic energy relationship: a critical literature appraisal. Journal of Hydrology, 261: 1–23.

Wischmeier W.H., Smith D.D. (1978): Predicting Rainfall Erosion Losses – a Guide to Conservation Planning. USDA Agricultural Research Service Handbook No. 537, Hyattsville, USDA.

Zanchi C., Torri D. (1980): Evalution of rainfall energy in central Italy. In: De Boodt M., Gabriels D. (eds.): Assessment of Erosion. Toronto, Wiley: 133–142.

Received for publication November 14, 2016
Accepted after corrections May 21, 2018
Published online July 9, 2018